International Journal of Electrical, Electronic and Communication Sciences
ISSN: 2517-9438
Vol:11, No:12, 2017

Energy Efficiency Analysis of Discharge Modes of an Adiabatic Compressed Air Energy Storage System

Shane D. Inder, Mehrdad Khamooshi

***Abstract*—**Efficient energy storage is a crucial factor in facilitating the uptake of renewable energy resources. Among the many options available for energy storage systems required to balance imbalanced supply and demand cycles, compressed air energy storage (CAES) is a proven technology in grid-scale applications. This paper reviews the current state of micro scale CAES technology and describes a micro-scale advanced adiabatic CAES (A-CAES) system, where heat generated during compression is stored for use in the discharge phase. It will also describe a thermodynamic model, developed in EES (Engineering Equation Solver) to evaluate the performance and critical parameters of the discharge phase of the proposed system. Three configurations are explained including: single turbine without preheater, two turbines with preheaters, and three turbines with preheaters. It is shown that the micro-scale A-CAES is highly dependent upon key parameters including; regulator pressure, air pressure and volume, thermal energy storage temperature and flow rate and the number of turbines. It was found that a micro-scale AA-CAES, when optimized with an appropriate configuration, could deliver energy input to output efficiency of up to 70%

***Keywords*—**CAES, adiabatic compressed air energy storage, expansion phase, micro generation, thermodynamic.

I. Introduction

THE energy requirements of a growing population and an increase in industrial activity has resulted in a reliance on energy dense, but ultimately unsustainable fossil fuels. Renewable energy generation is a favourable alternative to the depletion of fossil fuel reserves and toxic emissions. There has been a paradigm shift towards renewable energy harvesting technologies in recent years. Cost effective, renewable energy harvesting and efficient energy storage systems are crucial pieces of the energy puzzle. A well-appointed electricity grid requires the deployment of storage technologies to alleviate peak power demand (and subsequent increase in CO_2 emissions) from existing grid-scale electricity production. With increasing uptake of domestic rooftop photovoltaic harvesting and micro wind turbine systems, levelling the intermittent renewable supply is also a growing issue. Energy storage methods for excess grid-scale electricity generation e.g. battery systems, pumped-hydro, large scale CAES, molten salt and flywheels are viable options in specific applications and with varying levels of efficiency. In a CAES system, ambient air is compressed and stored under pressure in a storage chamber. When electricity is required, the air is expanded through an air-motor or turbine, rotating a generator to produce electricity. In an A-CAES the heat by-product of compression is transferred into a thermal energy storage. During expansion/generation phase, the pressurized air is heated prior to expansion through each turbine or air-motor stage, using the thermal energy storage.

CAES systems have been widely discussed, [1]-[5] with a focus on large-scale systems utilising caverns or disused mines [6]-[9]. Most residential/domestic renewable energy harvested from photovoltaic or micro-turbines, generates only a few kilowatts. Research on micro-scale energy storage systems almost exclusively centers on battery storage technologies. The A-CAES system proposed in this paper is considerably smaller than CAES designs for large-scale renewable energy power plants. This study attempts to review the current status of micro-scale CAES and A-CAES, and how they integrate to residential/domestic renewable energy systems.

Maia et al. [10] conducted an experimental study on a low cost micro-CAES which was made by an automotive turbocharger, and also included a generator, an electrical circuit, and a lubricating system. The proposed system could reach 45% input to output efficiency during operation, with ambient air temperature and without external sources of heat. Chen et al. [11] discussed the application of a zero-carbon-emission micro Energy Internet (ZCE-MEI) architecture by incorporating non-supplementary fired compressed air energy storage (NSF-CAES) hub. A hybrid control strategy based on the maximum power point tracking and maximum efficiency point tracking of micro-scale CAES was proposed by Zhang et al. [12]. The application of CAES in multi-generation cycles was discussed by Vollaro et al. [13]. A relatively small, 3 kWh of storage utilizing compressed-air with a capacity of 1 m^3 and pressure of 50 bar was used to produce electrical and thermal energy. During the discharge phase, a round-trip of 52% was measured. The thermodynamic assessment of a tri-generative micro CAES shows that the performance of the system significantly influenced by some operating and design parameters [14].

The development of a micro-CAES system for thermal and electrical energy for both residential and non-residential user was proposed by Tallini et al. [15]. For residential users the model CAES 1 (3 kW for about 3 hours), for non-residential users the model CAES 2 (6 kW for about 2 hours) was considered. The economic analysis showed that the payback period for CAES+PV is five years.

Shane D. Inder is with Department of Industrial Design and Innovation, Faculty of Design and Creative Technologies, Auckland University of Technology, Auckland, New Zealand (e-mail: shane.inder@aut.ac.nz).

Mehrdad Khamooshi is with the Department of Mechanical Engineering, Faculty of Design and Creative Technologies, Auckland University of Technology, Auckland, New Zealand (e-mail: mehrdad.khamooshi@aut.ac.nz).

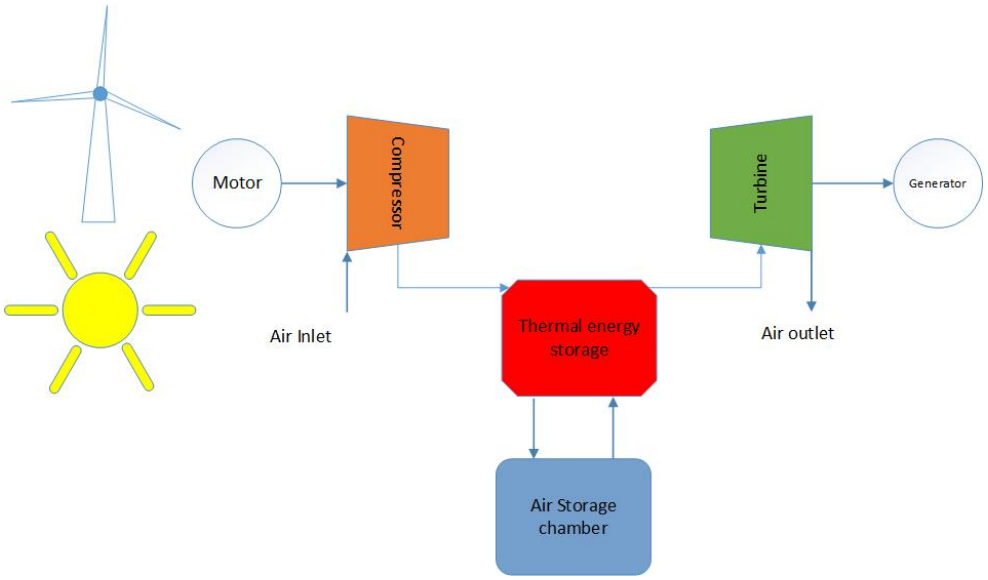

Fig. 1 Schematic view of A-CAES

The application of scroll expander in micro-CAES was examined in [16]. The results demonstrated that the energy conversion efficiency varies from 23% to 36% at the air supply pressure of 0.35 to 0.65 MPa, indicating that it is proportional to the air supply pressure. The performance of single stage system with air preheater, two stage without air preheating, and hydrogen energy system was compared with respect to their efficiency and financial viability. It was found out that the two-stage system is 2.5% more efficient compared to the hydrogen storage system [17].

A micro-CAES system with isothermal compression and expansion processes is a very effective system for distributed power networks. This system is combination of energy storage generation, and air-cycle heating and cooling system, with energy density feasible for distributed energy storage system and a good efficiency due to the multipurpose system [18].

An initial review indicates limited literature focusing on analysis of performance characteristics of micro-scale CAES systems. Micro-CAES is an adaptable solution for distributed future power networks and it is essential to investigate and optimize the performance of discharge mode of the system to use the energy stored in the tank efficiently. It is possible to build several different types of micro A-CAES systems based on expansion processes. This study presents three different configurations for assumed condition of compression process. A thermodynamic analysis is performed for all three configurations to identify the effects of some parameters such as the turbine efficiency, regulator pressure, heat exchanger efficiency, storage pressure, and storage volume on the amount of generated power.

II. Alternative Configurations of Expansion Process for Micro A-CAES

During times of electricity demand, the air is drawn from the tank through a pressure regulator and then it enters the expansion process. The differences between the proposed systems are in the number of turbines and heat exchangers.

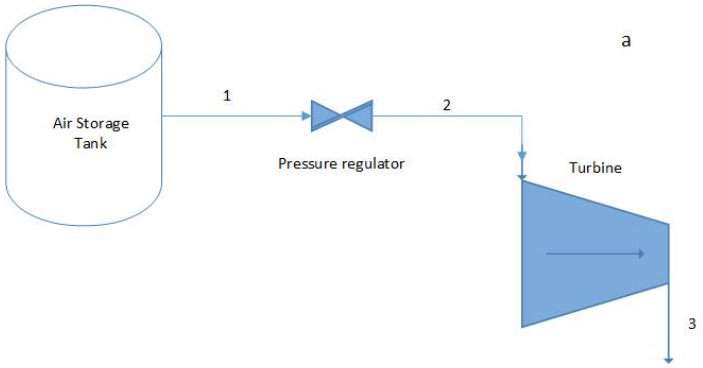

(a) Configuration 1

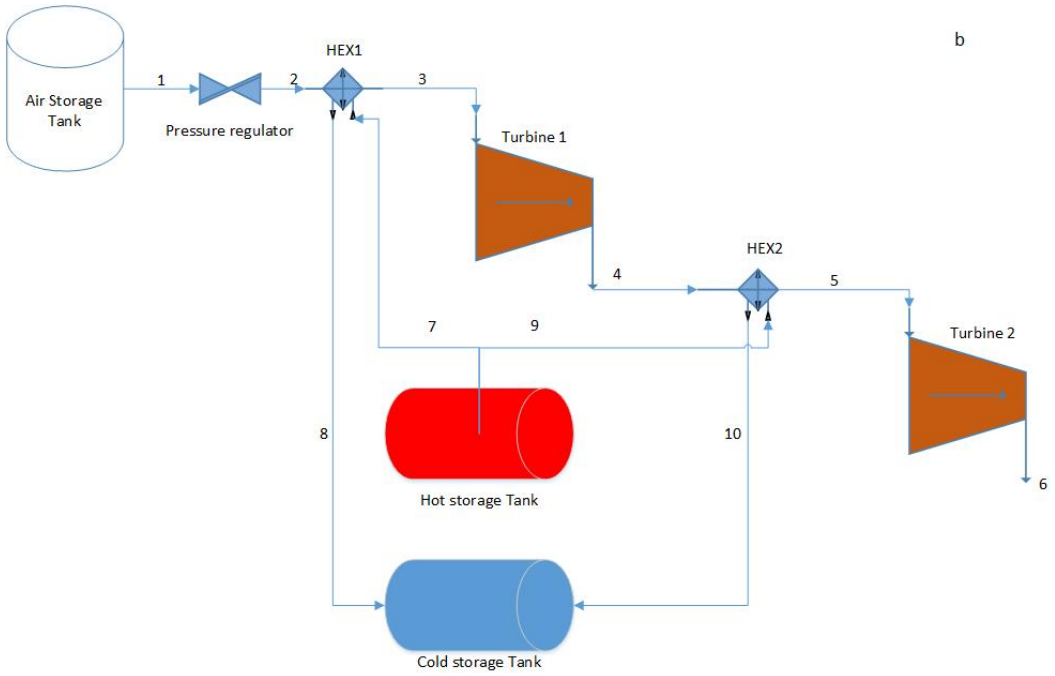

(b) Configuration 2

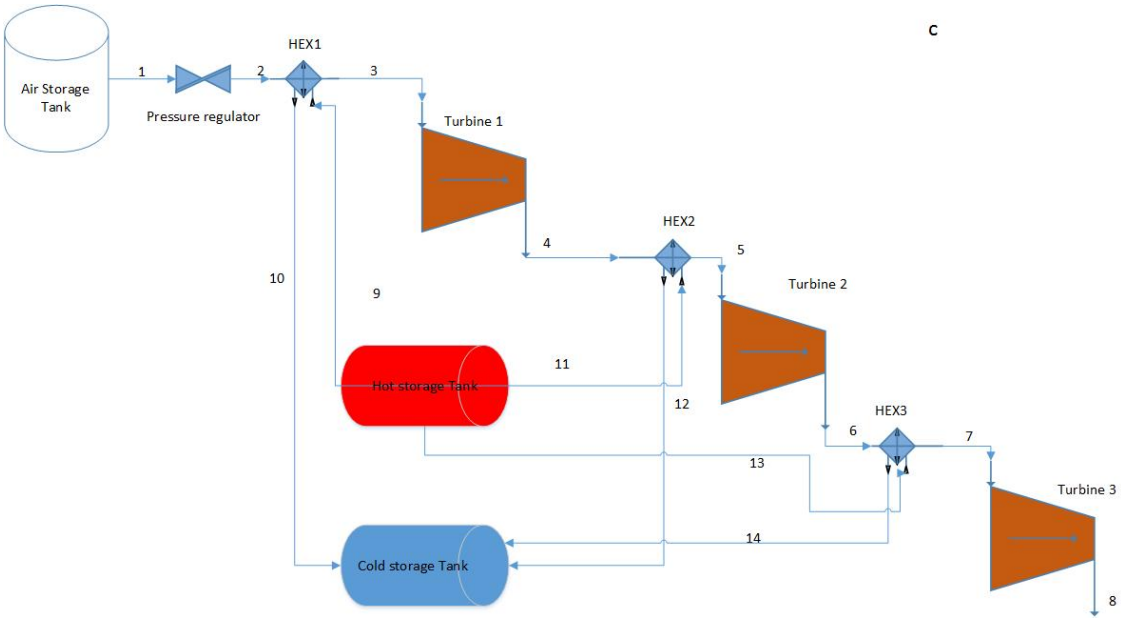

(c) Configuration 3

Fig. 2 Three configurations of A-CAES expansion process

III. Thermodynamic Modelling

The thermodynamics model used for the simulation of the A-CAES discharge processes is described, highlighting assumptions and parameters. Each component of the considered system has been treated as a control volume and the principles of mass and energy conservation are applied to it. EES software is used for solving the equations [19]:

A. Assumptions

The following assumptions have been made in the analysis:

i. Changes in kinetic and potential energies are neglected.
ii. The system is in thermodynamic equilibrium and all the processes are assumed to be steady flow processes.
iii. Some proper values of effectiveness are considered for the heat exchangers.

iv. Varying and constant pressure are considered for the air storage tank. So in varying pressure the process ends when the tank pressure reaches the turbine inlet.
v. Air obeys the ideal gas law.

B. Performance Evaluation

TABLE I
INPUT PARAMETERS

Parameter	Symbol	Value
Isentropic turbine efficiency	%	10-80
Volume of the tank	M3	0.25
Initial pressure of the tank	Bar	200
Heat exchanger efficiency	%	80
Environment temperature	K	298.15
Environment pressure	Bar	1
Regulator pressure	Bar	8
Hot storage tank temperature	K	427
Turbines pressure ratio		1/2
Output pressure of last turbine		P_0

Volumetric energy density of the system is defined as the ratio of the total work produced to the volume of the consumable energy source (volume of the air storage tank):

$$VED = \frac{W_t}{V} \quad (1)$$

where W_t is the total output of the system and V is the air storage tank volume.

Heat exchanger effectiveness ε defined by Kays and London [20] is introduced for the evaluation of heat exchange process (2):

$$\varepsilon = \frac{C_{p1}m_1(T_{in1}-T_{out1})}{(C_pm)_{min}(T_{in1}-T_{in2})} = \frac{C_{p2}m_2(T_{out2}-T_{in2})}{(C_pm)_{min}(T_{in1}-T_{in2})} \quad (2)$$

where subscript 1 denotes the hot fluid and subscript 2 denotes the cold fluid.

The mass balance can be expressed as:

$$\sum \dot{m}_{in} - \sum \dot{m}_{out} = 0 \quad (3)$$

Constant tank pressure:

$$\dot{m}_{out} = \dot{m}_1 \quad (4)$$

Varying tank pressure:

$$\dot{m}_{out} = \dot{m}_1 - \dot{m}_2 \quad (5)$$

State 2, the state of the air in the tank at the end of process, is specified by the temperature, T2=T0 and pressure P2=Pt,in. The process ends when the tank pressure reaches the turbine inlet pressure.

The first law of thermodynamics yields the energy balance for each component as:

$$\sum(\dot{m}h)_{in} - \sum(\dot{m}h)_{out} + \dot{Q}_{cv} + \dot{W}_{cv} = 0 \quad (6)$$

Power generation including efficiency for each turbine equals:

$$W = m_{out}\eta_{turbine}\frac{k}{k-1}R_AT_{in}[(\frac{P_{out}}{P_{in}})^{\frac{k-1}{k}} - 1] \quad (7)$$

where K is isentropic efficiency equals to 1.4 and R_A = 287.06 J/kg K gas constant.

C. Validation

The available data in literature were used to validate the simulation results. For first configuration, the results reported in [21] are used. The conditions and assumptions used are as follows:

i. Air is stored in a V=2 litre compressed air tank.
ii. The air initially charged to 2400 psi.
iii. The isentropic efficiency of the turbine is 0.75.
iv. The process ends when the tank pressure reaches the turbine inlet pressure.

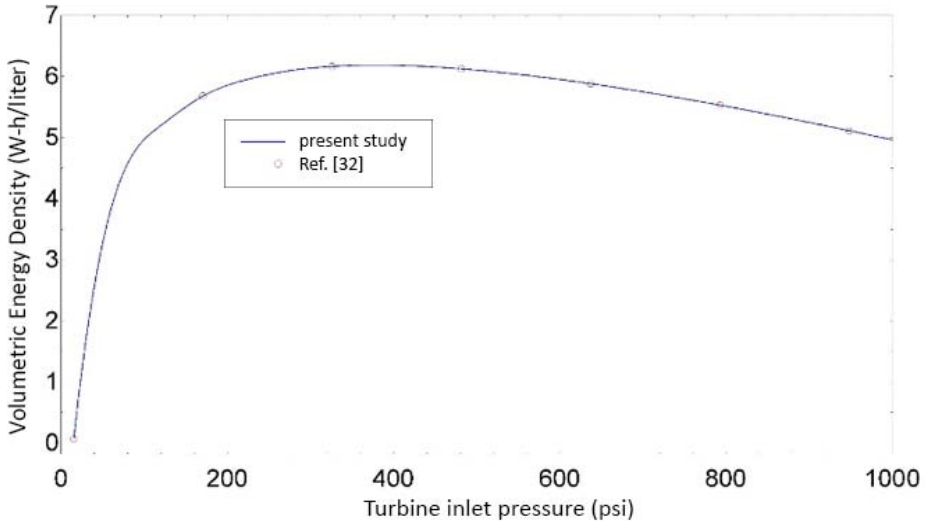

Fig. 3 Effect of turbine inlet pressure on VED for configuration 1a in comparison with that of reported in [21]

Fig. 3 shows the effect of turbine inlet pressure on the COP of the same system. The consistency and similarity between the obtained result of the current work and the results from the case study in [21] show the validation of the system.

IV. Results and Discussion

The impacts of the Preg on VED of different configurations with varying and constant tank pressure are presented in Fig. 4. It is clear that the cycle performs better under constant tank pressure. Based on (4) and (5) it can be concluded that the mass of air that leaves the tank and passes the turbine is greater in constant pressure compared to the varying pressure. The volumetric energy density of configurations 1-3 with constant tank pressure at Preg=40 bar are evaluated to be 0.012625, 0.019977 and 0.022307 which can deliver 2.525, 3.9954 and 4.6414 kW-hr respectively.

The VED and Output of configurations 1-3 were investigated with respect to Preg at different isentropic efficiencies as shown in Figs. 5-7. The outputs of the configurations 2 and 3 are considerably higher than configuration 1 due to existence of additional turbine and increased inlet temperature (utilizing Thermal Energy Storage and pre and inter-stage heat exchangers). In the case of configuration 3 the output increase is noticeable. The increase is caused by the partitioning of the second expansion stage (of configuration 2) into three stages.

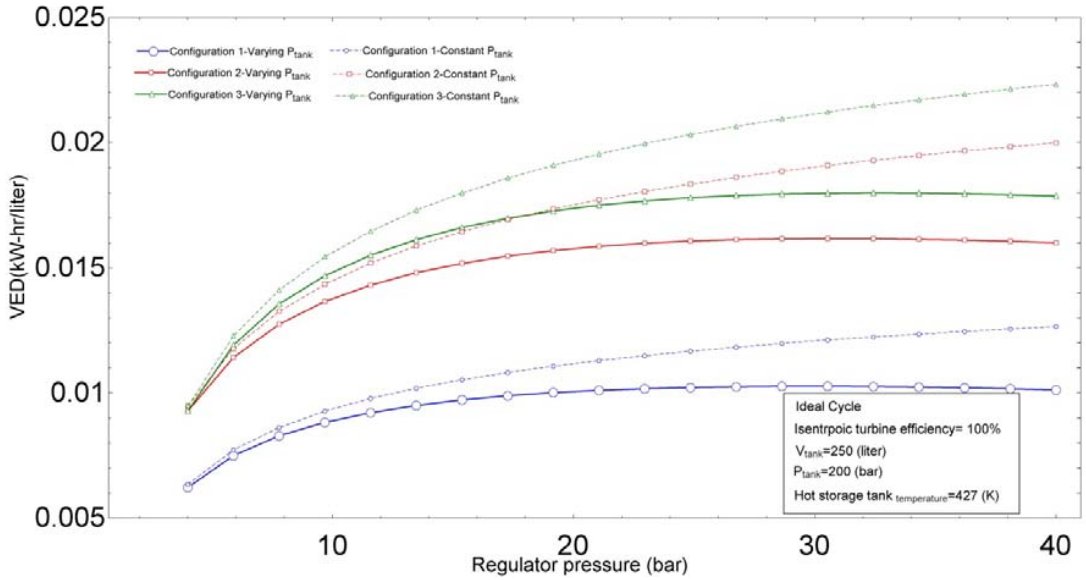

Fig. 4 Effect of Preg on VED for different configurations with constant and varying tank pressure

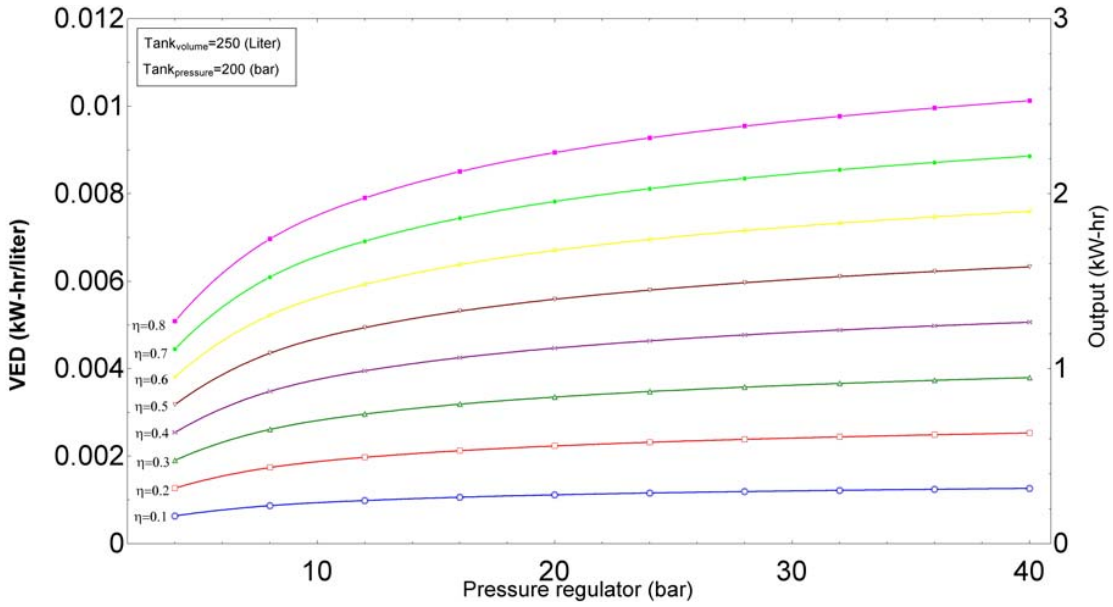

Fig. 5 Effect of Preg on VED and output of configuration 1 at different turbine isentropic efficiencies

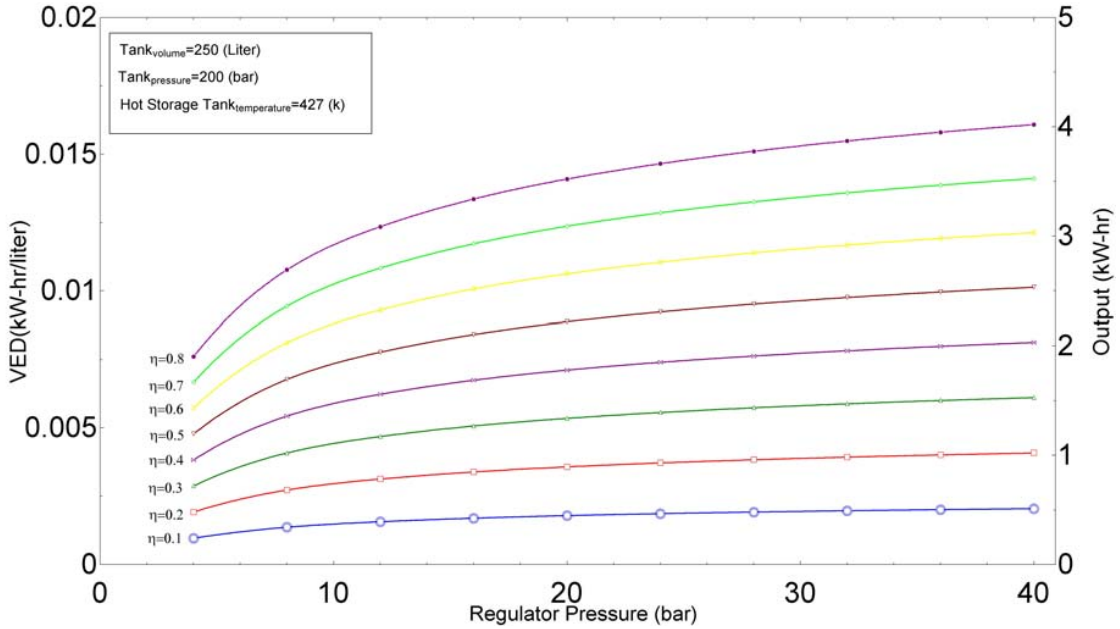

Fig. 6 Effect of Preg on VED and output of configuration 2 at different turbine isentropic efficiencies

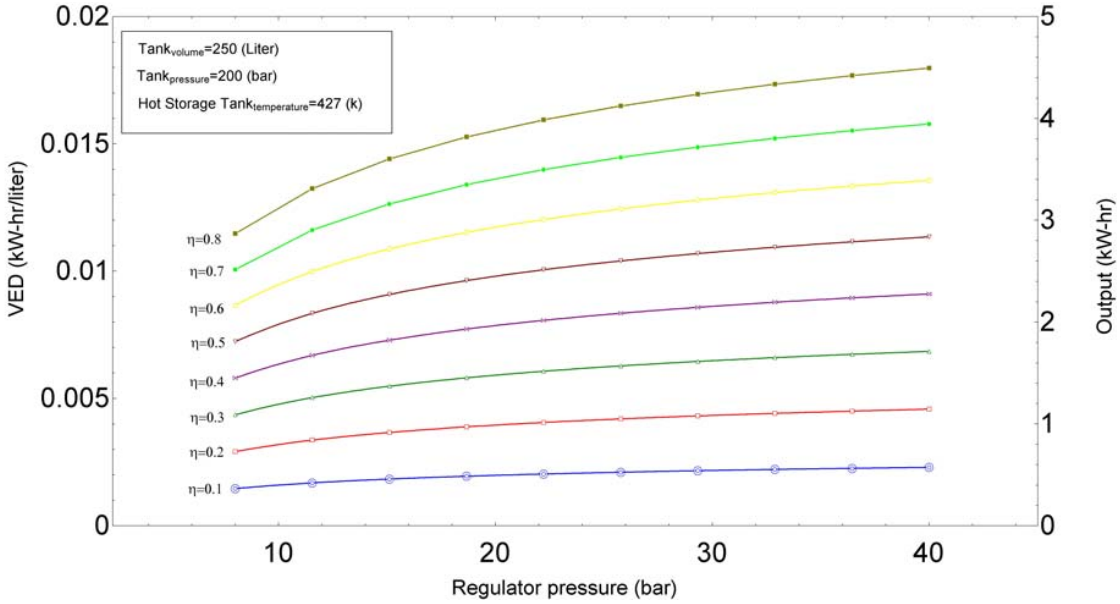

Fig. 7 Effect of Preg on VED and output configuration 3 at different turbine isentropic efficiencies.

It has been demonstrated that the total generated work increases as the inlet temperature of the turbine increases. An increase in inlet temperature (utilizing TES and pre and inter-stage heat exchangers) increases the overall output of the system. The effect of TES temperature on the output of the configuration 2 and 3 is shown in Fig. 3. Increasing the temperature of TES can improve the total output of the configurations 2 and 3 by 23 and 25% respectively.

The performance of the discharge cycle of a micro A-CAES not only depends on the discharge configuration but also variables such as air storage tank pressure and volume, significant for increasing the output of the system. Figs. 4 and 5 present the effect of V_{tank} and P_{tank} on the output of the three different configurations.

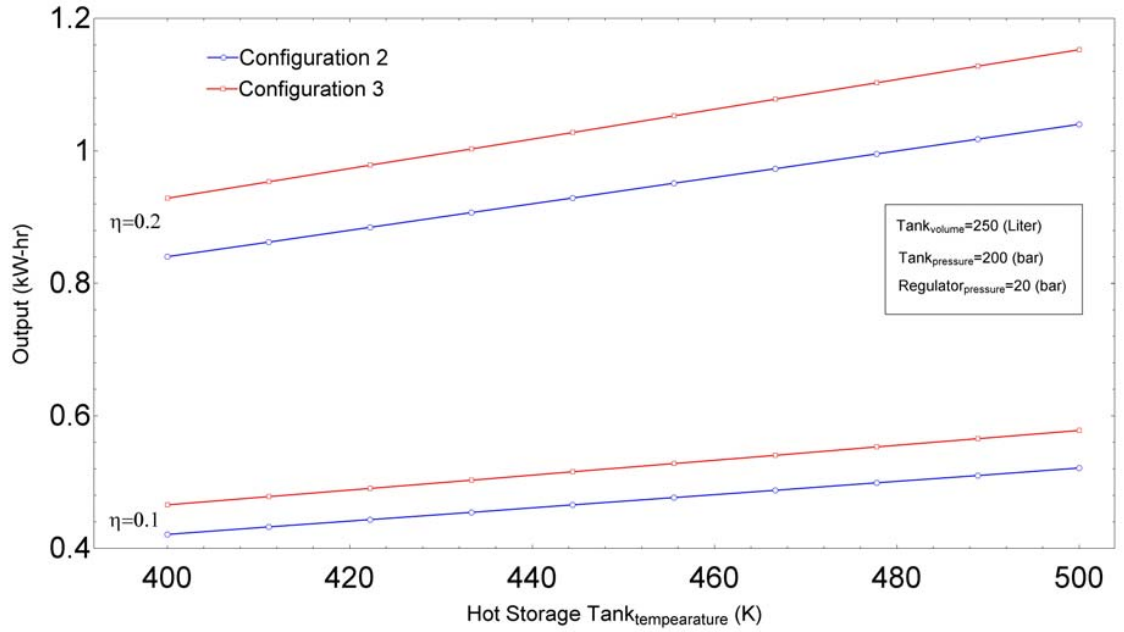

Fig. 8 Effect of hot storage tank temperature on output of the configurations 2 and 3 at different turbine isentropic efficiencies

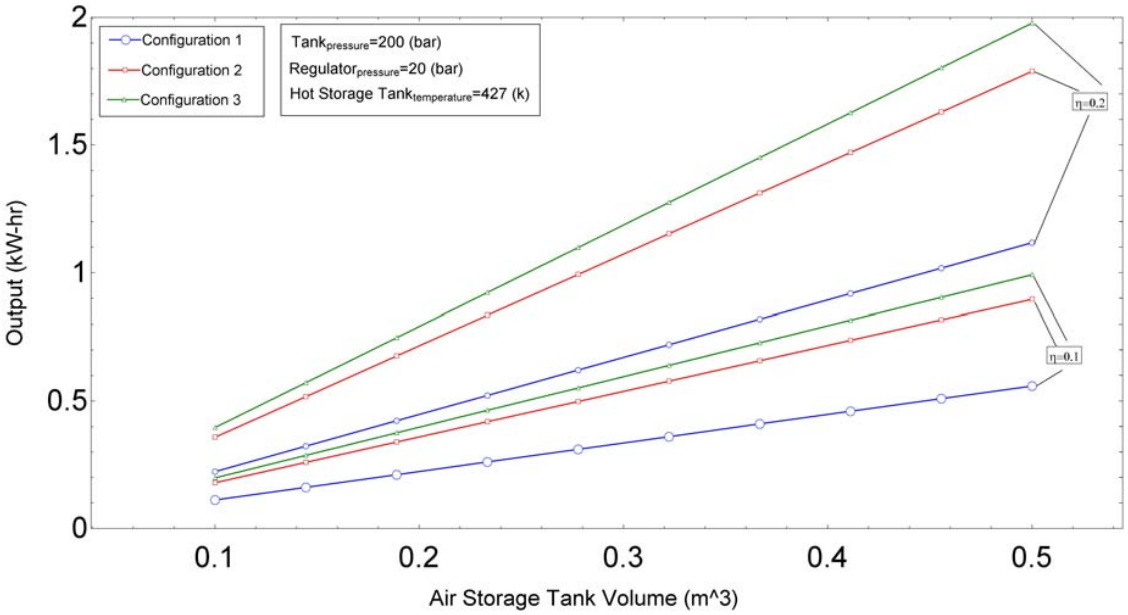

Fig. 9 Effect of air storage tank volume on output of the all configurations at different turbine isentropic efficiencies

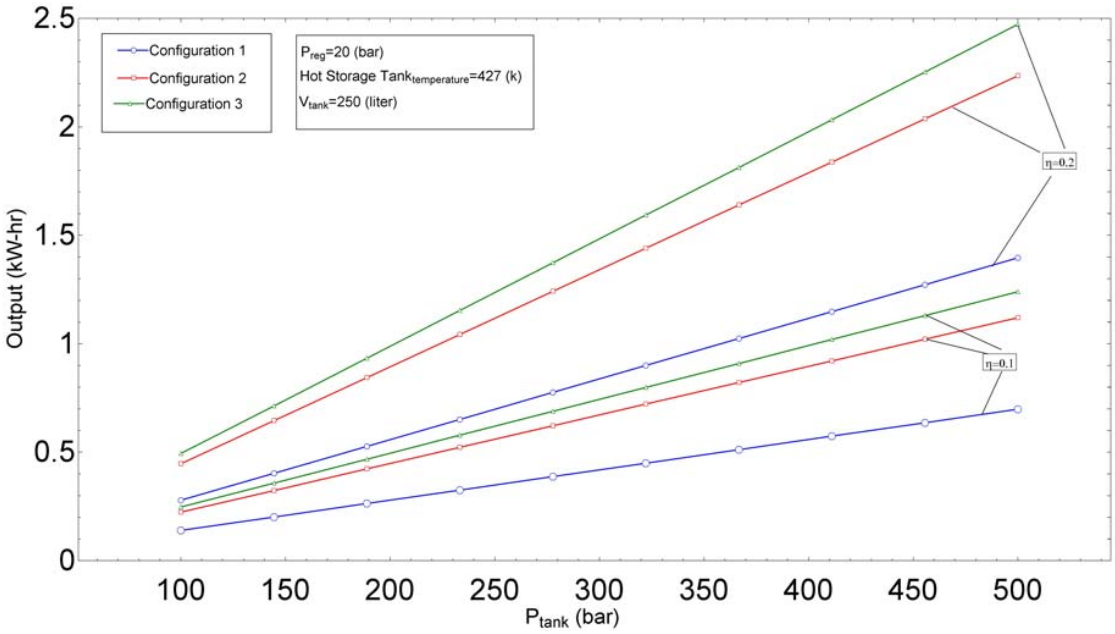

Fig. 5 Effect of air storage tank pressure on output of the all configurations at different turbine isentropic efficiencies

The outputs of all configurations are outlined in Tables II-IV.

TABLE II
PERFORMANCE CHARACTERISTICS OF CONFIGURATION 1 WITH DIFFERENT REGULATOR PRESSURES

$\eta_{Turbine}$	P_{reg}	V_{tank} (liter)	P_{tank} (bar)	VED (kW-hr)	Output (kW-hr)
0.1	10	250	200	0.000936	0.2342
0.1	15	250	200	0.001047	0.2617
0.1	20	250	200	0.001181	0.2794
0.2	10	250	200	0.001874	0.4685
0.2	15	250	200	0.002094	0.5235
0.2	20	250	200	0.002235	0.5588
0.3	10	250	200	0.002811	0.7027
0.3	15	250	200	0.003141	0.7852
0.3	20	250	200	0.003353	0.8382
0.4	10	250	200	0.003748	0.9369
0.4	15	250	200	0.004188	1.047
0.4	20	250	200	0.00447	1.118
0.5	10	250	200	0.004685	1.171
0.5	15	250	200	0.005235	1.309
0.5	20	250	200	0.005588	1.397
0.6	10	250	200	0.005622	1.405
0.6	15	250	200	0.006282	1.57
0.6	20	250	200	0.006706	1.676
0.7	10	250	200	0.006558	1.64
0.7	15	250	200	0.007329	1.832
0.7	20	250	200	0.007823	1.956

TABLE III
PERFORMANCE CHARACTERISTICS OF CONFIGURATION 2 WITH DIFFERENT REGULATOR PRESSURES

$\eta_{Turbine}$	P_{reg} (bar)	$T_{hot\ storage\ tank}$ (k)	V_{tank} (liter)	P_{tank} (bar)	VED (kW-hr)	Output (kW-hr)
0.1	10	427	250	200	0.001482	0.3705
0.1	15	427	250	200	0.001671	0.4179
0.1	20	427	250	200	0.001793	0.4483
0.2	10	427	250	200	0.002957	0.7392
0.2	15	427	250	200	0.003335	0.8337
0.2	20	427	250	200	0.003577	0.8943
0.3	10	427	250	200	0.004425	1.106
0.3	15	427	250	200	0.00499	1.247
0.3	20	427	250	200	0.005352	1.338
0.4	10	427	250	200	0.005886	1.472
0.4	15	427	250	200	0.006636	1.659
0.4	20	427	250	200	0.007118	1.78
0.5	10	427	250	200	0.00734	1.835
0.5	15	427	250	200	0.008275	2.069
0.5	20	427	250	200	0.008875	2.219
0.6	10	427	250	200	0.008787	2.197
0.6	15	427	250	200	0.009905	2.476
0.6	20	427	250	200	0.01062	2.656
0.7	10	427	250	200	0.01023	2.557
0.7	15	427	250	200	0.01153	2.882
0.7	20	427	250	200	0.01236	3.09

TABLE IV
PERFORMANCE CHARACTERISTICS OF CONFIGURATION 3 WITH DIFFERENT REGULATOR PRESSURES

$\eta_{turbine}$	P_{reg} (bar)	$T_{hot\ storage\ tank}$ (k)	V_{tank} (liter)	P_{tank} (bar)	VED (kW-hr)	Output (kW-hr)
0.1	10	427	250	200	0.001602	0.4004
0.1	15	427	250	200	0.001835	0.4587
0.1	20	427	250	200	0.001984	0.4961
0.2	10	427	250	200	0.003195	0.7987
0.2	15	427	250	200	0.003658	0.9146
0.2	20	427	250	200	0.003957	0.9892
0.3	10	427	250	200	0.004779	1.195
0.3	15	427	250	200	0.005472	1.368
0.3	20	427	250	200	0.005917	1.479
0.4	10	427	250	200	0.006354	1.589
0.4	15	427	250	200	0.007274	1.818
0.4	20	427	250	200	0.007866	1.966
0.5	10	427	250	200	0.007921	1.98
0.5	15	427	250	200	0.009066	2.266
0.5	20	427	250	200	0.009802	2.451
0.6	10	427	250	200	0.009479	2.37
0.6	15	427	250	200	0.01085	2.712
0.6	20	427	250	200	0.01173	2.932
0.7	10	427	250	200	0.01103	2.757
0.7	15	427	250	200	0.01262	3.154
0.7	20	427	250	200	0.01364	3.41

V. CONCLUSION

Micro-scale CAES has been shown to be an efficient and clean solution for energy storage challenges in residential buildings. A thermodynamic analysis of three different configurations of the discharge phase of a micro-scale A-CAES system was conducted. The study aimed to evaluate the performance of the system under various pressure and temperature conditions. Based on the analysis, the following conclusions are drawn:

- The higher pressure regulator is, the higher VED and output will be.
- The performance of the cycles not only depends on the discharging process but also on variables such as air storage tank pressure and volume.
- Increasing the input temperature using heat from stored thermal energy reservoir to configuration 1 increases the output and VED of the cycle.
- Configuration 3 has the highest VED and output compared to the first and second configurations.
- When considering an ideal turbine (100% isentropic efficiency) and input parameters (Table I) configurations 1-3 can deliver 2.525, 3.9954 and 4.6414 kW-hr respectively.

ACKNOWLEDGMENT

This research was conducted with support and funding from the Energy Education Trust of New Zealand.

REFERENCES

[1] Rohit, A.K., K.P. Devi, and S. Rangnekar, *An overview of energy storage and its importance in Indian renewable energy sector: Part I – Technologies and Comparison.* Journal of Energy Storage, 2017. 13 (Supplement C): p. 10-23.

[2] Gasia, J., L. Miró, and L.F. Cabeza, *Review on system and materials requirements for high temperature thermal energy storage. Part 1: General requirements.* Renewable and Sustainable Energy Reviews, 2017. 75: p. 1320-1338.

[3] Hoque, M.M., et al., *Battery charge equalization controller in electric vehicle applications: A review.* Renewable and Sustainable Energy Reviews, 2017. 75: p. 1363-1385.

[4] Nkhonjera, L., et al., *A review of thermal energy storage designs, heat storage materials and cooking performance of solar cookers with heat storage.* Renewable and Sustainable Energy Reviews, 2017. 75: p. 157-167.

[5] Thieblemont, H., et al., *Predictive control strategies based on weather forecast in buildings with energy storage system: A review of the state-of-the art.* Energy and Buildings, 2017. 153: p. 485-500.

[6] Bitaraf, H. and S. Rahman, *Reducing Curtailed Wind Energy through Energy Storage and Demand Response.* IEEE Transactions on Sustainable Energy, 2017.

[7] Huang, Y., et al. *Techno-economic Modelling of Large Scale Compressed Air Energy Storage Systems*. in *Energy Procedia*. 2017.

[8] Kapila, S., A.O. Oni, and A. Kumar, *The development of techno-economic models for large-scale energy storage systems.* Energy, 2017. 140: p. 656-672.

[9] Shahinzadeh, H., et al. *Simultaneous operation of near-to-sea and off-shore wind farms with ocean renewable energy storage*. in *4th Iranian Conference on Renewable Energy and Distributed Generation, ICREDG 2016*. 2017.

[10] Maia, T.A.C., et al., *Experimental performance of a low cost micro-CAES generation system.* Applied Energy, 2016. 182: p. 358-364.

[11] Li, R., et al., *Optimal dispatch of zero-carbon-emission micro Energy Internet integrated with non-supplementary fired compressed air energy storage system.* Journal of Modern Power Systems and Clean Energy, 2016. 4(4): p. 566-580.

[12] Zhang, L., Q. Luo, and Q. An, *Control strategy of electromechanical system of hydro-pneumatic compressed air storage system.* Diangong Jishu Xuebao/Transactions of China Electrotechnical Society, 2016. 31(14): p. 67-74.

[13] De Lieto Vollaro, R., et al. *Energy and thermodynamical study of a small innovative compressed air energy storage system (micro-CAES)*. in *Energy Procedia*. 2015.

[14] Facci, A.L., et al., *Trigenerative micro compressed air energy storage: Concept and thermodynamic assessment.* Applied Energy, 2015. 158: p. 243-254.

[15] Tallini, A., A. Vallati, and L. Cedola, *Applications of Micro-CAES Systems: Energy and Economic Analysis.* Energy Procedia, 2015. 82 (Supplement C): p. 797-804.

[16] Xinghua, Y., et al., *Simulation and experimental research on energy conversion efficiency of scroll expander for micro-Compressed Air Energy Storage system.* International Journal of Energy Research, 2014. 38(7): p. 884-895.

[17] Karellas, S. and N. Tzouganatos, *Comparison of the performance of compressed-air and hydrogen energy storage systems: Karpathos island case study.* Renewable and Sustainable Energy Reviews, 2014. 29: p. 865-882.

[18] Kim, Y.M. and D. Favrat, *Energy and exergy analysis of a micro-compressed air energy storage and air cycle heating and cooling system.* Energy, 2009. 35(1): p. 213-220.

[19] Klein, S.A., Engineering Equation Solver (EES), 2011.

[20] Shah, R.K. and D.P. Sekulic, Fundamentals of Heat Exchanger Design, 2003.

[21] Klein, S.A. and G. Nellis, *Thermodynamics*. 2012: Cambridge University Press.